Article

Cell Reports

Aberrant Compartment Formation by HSPB2 Mislocalizes Lamin A and Compromises Nuclear Integrity and Function

Graphical Abstract

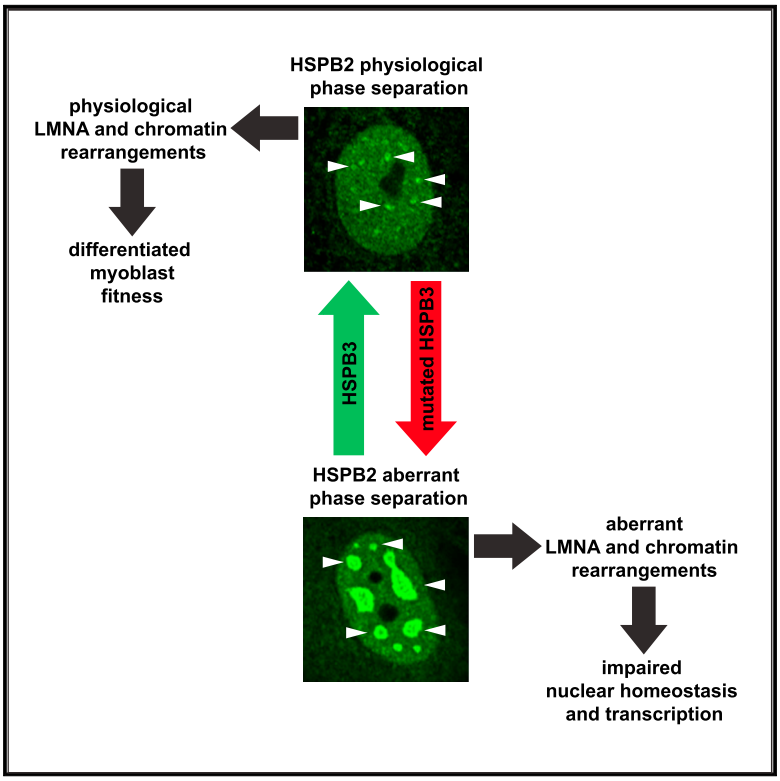

Authors

Federica F. Morelli, Dineke S. Verbeek, Jessika Bertacchini, ..., Rossella Tupler, Simon Alberti, Serena Carra

Correspondence

serena.carra@unimore.it

In Brief

Morelli et al. show that, in mammalian cells, HSPB2 forms liquid-like nuclear compartments that affect lamin A localization and mobility, with detrimental consequences for chromatin organization and nuclear integrity. Aberrant compartment formation by HSPB2 is regulated by HSPB3, but not by two identified HSPB3 mutants linked to myopathy.

Highlights

- HSPB2 undergoes concentration-dependent liquid-liquid phase separation in cells
- HSPB2 phase separation requires its intrinsically disordered C-terminal tail
- Aberrant HSPB2 phase separation mislocalizes lamin A
- HSPB3, but not two HSPB3 myopathy mutants, inhibits HSPB2 phase separation

Morelli et al., 2017, Cell Reports *20*, 2100–2115
August 29, 2017
http://dx.doi.org/10.1016/j.celrep.2017.08.018

OPEN ACCESS
CellPress

Cell Reports
Article

Aberrant Compartment Formation by HSPB2 Mislocalizes Lamin A and Compromises Nuclear Integrity and Function

Federica F. Morelli,[1] Dineke S. Verbeek,[2,11] Jessika Bertacchini,[1,11] Jonathan Vinet,[1] Laura Mediani,[1] Sandra Marmiroli,[3] Giovanna Cenacchi,[4] Milena Nasi,[3] Sara De Biasi,[3] Jeanette F. Brunsting,[5] Jan Lammerding,[6] Elena Pegoraro,[7] Corrado Angelini,[8] Rossella Tupler,[9] Simon Alberti,[10] and Serena Carra[1,12,*]

[1]Department of Biomedical, Metabolic and Neuronal Sciences, University of Modena and Reggio Emilia, and Center for Neuroscience and Neurotechnology, 41125 Modena, Italy
[2]Department of Genetics, University of Groningen, University Medical Center Groningen, 9713 AV Groningen, the Netherlands
[3]Department of Surgery, Medicine, Dentistry and Morphology, University of Modena and Reggio Emilia, 41125 Modena, Italy
[4]Department of Biomedical and Neuromotor Sciences, University of Bologna, 40126 Bologna, Italy
[5]Department of Cell Biology, University of Groningen, University Medical Center Groningen, 9713 AV Groningen, the Netherlands
[6]Meinig School of Biomedical Engineering, Weill Institute for Cell and Molecular Biology, Cornell University, Ithaca, NY 14853-7202, USA
[7]Department of Neurosciences, University of Padua, 35122 Padua, Italy
[8]IRCCS S. Camillo Hospital, 30126 Lido Venice, Italy
[9]Department of Life Sciences, University of Modena and Reggio Emilia, 41125 Modena, Italy
[10]Max Planck Institute of Molecular Cell Biology and Genetics, 01307 Dresden, Germany
[11]These authors contributed equally
[12]Lead Contact
*Correspondence: serena.carra@unimore.it
http://dx.doi.org/10.1016/j.celrep.2017.08.018

SUMMARY

Small heat shock proteins (HSPBs) contain intrinsically disordered regions (IDRs), but the functions of these IDRs are still unknown. Here, we report that, in mammalian cells, HSPB2 phase separates to form nuclear compartments with liquid-like properties. We show that phase separation requires the disordered C-terminal domain of HSPB2. We further demonstrate that, in differentiating myoblasts, nuclear HSPB2 compartments sequester lamin A. Increasing the nuclear concentration of HSPB2 causes the formation of aberrant nuclear compartments that mislocalize lamin A and chromatin, with detrimental consequences for nuclear function and integrity. Importantly, phase separation of HSPB2 is regulated by HSPB3, but this ability is lost in two identified HSPB3 mutants that are associated with myopathy. Our results suggest that HSPB2 phase separation is involved in reorganizing the nucleoplasm during myoblast differentiation. Furthermore, these findings support the idea that aberrant HSPB2 phase separation, due to HSPB3 loss-of-function mutations, contributes to myopathy.

INTRODUCTION

Mammals have ten small heat shock proteins (HSPBs: HSPB1–HSPB10), which belong to the family of molecular chaperones. While some HSPBs are ubiquitously expressed and have been widely studied, such as HSPB1 and HSPB5, others are expressed only in few tissues and are poorly characterized (Boncoraglio et al., 2012). One example of the latter category is HSPB2, which is expressed in differentiated skeletal and cardiac muscle cells, where it can form a complex with HSPB3 (den Engelsman et al., 2009; Sugiyama et al., 2000). Defects in HSPB2 deregulate the expression of metabolic and mitochondrial genes in response to pressure overload in the mammalian heart (Ishiwata et al., 2012). Moreover, myocardial overexpression of HSPB2 protects, with yet-unknown mechanisms, cardiomyocytes from ischemia (Grose et al., 2015), a pathological condition characterized by early transcriptional changes aimed at promoting damage repair (Wechsler et al., 1994). However, how changes in HSPB2 levels affect gene expression is still unknown.

From a structural point of view, HSPBs are composed of a well-conserved α-crystallin domain (ACD) and less conserved N- and C-terminal domains. HSPBs are disordered proteins, which contain domains of low complexity, referred to as intrinsically disordered regions (IDRs) (Sudnitsyna et al., 2012).

Over the past six years, proteins with low-complexity IDRs have been intensively studied, because they are able to drive the formation of liquid droplets in cells via a process known as liquid-liquid phase separation (Zhu and Brangwynne, 2015; Banani et al., 2017). These liquid droplets have been proposed to function as membrane-less organelles (MLOs) (Zhu and Brangwynne, 2015; Banani et al., 2017). Examples of MLOs are nuclear bodies such as nucleoli, promyelocytic leukemia protein (PML) bodies, Cajal bodies, speckles and paraspeckles, and cytoplasmic ribonucleoprotein particles, such as stress granules and P bodies (Banani et al., 2017). These MLOs differ in size, number, and composition, but they are all highly dynamic and show liquid-like behavior.

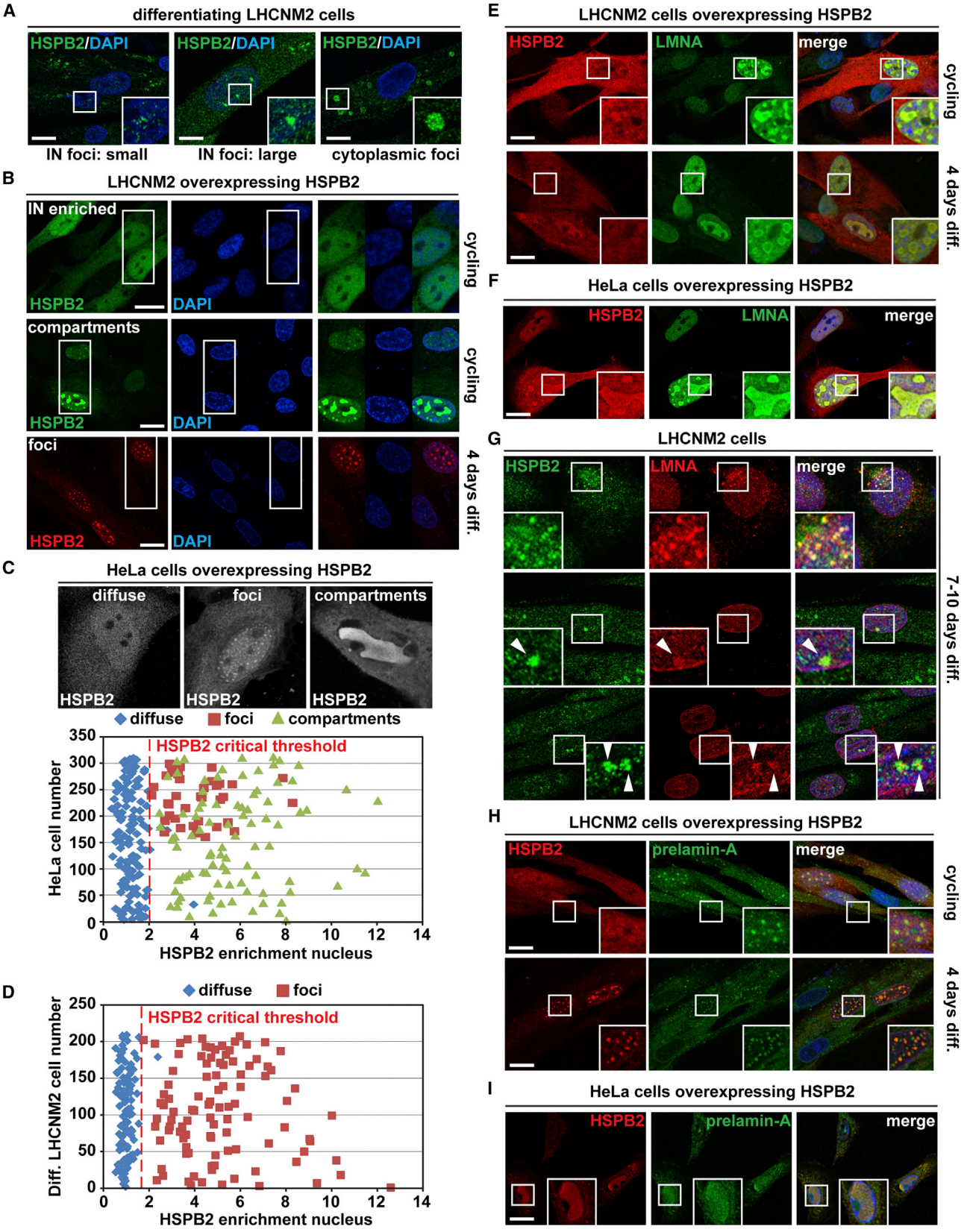

(legend on next page)

Our understanding of the signals that drive self-assembly of MLOs in mammalian cells is still limited; however, it is known that specific stressors and an increase in the concentration of IDR-containing proteins can induce the formation of liquid droplets in the cytoplasm (Patel et al., 2015) and nucleus (Schmidt and Rohatgi, 2016). For example, overexpression of TDP-43 drives the assembly of nuclear droplets that segregate portions of the nucleoplasm and regulate specific nuclear functions (Schmidt and Rohatgi, 2016).

Recruitment of HSPBs into MLOs was documented previously. For example, HSPB1, HSPB5, and HSPB7 are recruited into nuclear speckles, which are splicing factor compartments (Bryantsev et al., 2007; van den IJssel et al., 2003; Vos et al., 2009), while HSPB8 and, to a lesser extent, HSPB1 are recruited inside cytoplasmic stress granules, ribonucleoprotein particles that store and protect mRNAs upon stress (Ganassi et al., 2016). What drives the recruitment of these HSPBs into MLOs and whether recruitment depends on the presence of IDRs in HSPBs are largely unknown. Moreover, direct evidence that members of the HSPB family can phase separate and form liquid droplets has not yet been provided.

Here, we demonstrate that, in differentiating myoblasts, HSPB2 forms cytoplasmic and nuclear spherical foci. While HSPB2 cytoplasmic foci partly colocalize with HSPB3, nuclear foci partly colocalize with the nuclear intermediate filament protein lamin-A/C (LMNA). LMNA exerts different nuclear functions, including the regulation of nuclear stability, genome organization, and transcription. Moreover, mutations in the *LMNA* gene cause skeletal and cardiac myopathy (Davidson and Lammerding, 2014). Overexpression of HSPB2 in several cell types, including human myoblasts, promotes HSPB2 assembly into cytoplasmic and nuclear compartments, which behave as liquid droplets. Aberrant phase separation of HSPB2 changes LMNA and chromatin distribution with detrimental consequences for nuclear function and integrity. Importantly, HSPB2 phase separation is negatively regulated by its binding partner HSPB3. Depletion of HSPB3 enhances HSPB2 compartmentalization, decreases myogenin expression, and leads to micronuclei formation. Finally, we identified two mutations in the *HSPB3* gene in myopathic patients. Both myopathy-linked mutations disrupt the binding of HSPB3 to HSPB2 and trigger phase separation of HSPB2 into aberrant compartments. Our data suggest that a developmentally regulated increase in HSPB2 concentration reorganizes nucleoplasmic LMNA distribution during myoblast differentiation. Deregulation of HSPB2 assembly, due to HSPB3 mutations, may contribute to myopathy.

RESULTS

HSPB2 Forms Intranuclear Compartments in Mammalian Cells

To gain insights in HSPB2 properties, we studied its expression and subcellular distribution in human immortalized myoblasts (LHCNM2 cells) (Zhu et al., 2007). Differentiation of myoblasts follows an ordered sequence of events. The first step is commitment to differentiation, with upregulation of the transcription factor myogenin, followed by cell-cycle arrest, cell migration, adhesion, and phenotypic differentiation. This goes along with expression of genes, coding for contractile proteins, and fusion of mononucleated cells into multinucleated myotubes (Andrés and Walsh, 1996).

To characterize our LHCNM2 cells, we compared the expression levels of myogenin and desmin, markers of myoblast differentiation. Myogenin mRNA and desmin protein were absent from cycling (non-differentiating) LHCNM2 cells; they were both induced during differentiation (Figures S1A and S1B) (Kaufman and Foster, 1988). In agreement with published data (Sugiyama et al., 2000), HSPB2 and HSPB3 mRNA and protein were undetectable in cycling LHCNM2 cells but upregulated during differentiation (Figures S1A and S1B).

Next, we performed an immunohistochemical analysis of cycling and differentiating human myoblasts. We found a surprising heterogeneity in HSPB2 subcellular localization. Seven days post-differentiation, we found many multinucleated cells with homogeneous distribution of HSPB2 and HSPB3 both in the cytoplasm and nuclei (Figure S1C). However, some cells showed nuclear foci containing HSPB2, but not HSPB3; also, the number and size of these HSPB2-containing foci varied from dozens of small foci to one or a few large nuclear structures (Figures 1A and S1C). After 10 days of differentiation, we found mono- and multinucleated cells with undetectable nuclear HSPB3 staining and nuclear HSPB2 foci and cells with cytoplasmic HSPB2 spherical foci that partly colocalized with HSPB3 (Figures 1A and S1C). Thus, during the early steps of myoblast differentiation, HSPB2 forms two types of structures: nuclear foci that do not colocalize with HSPB3, in mono- and multinucleated cells, and cytoplasmic spherical foci that partly colocalize with HSPB3. The functional significance of these HSPB2 nuclear and cytoplasmic foci is currently unknown.

Figure 1. HSPB2 Forms Nuclear Compartments that Sequester LMNA in Cells

(A) Immunofluorescence on differentiating (diff.) LHCNM2 cells showing HSPB2 and DAPI. IN, intranuclear.

(B) Immunofluorescence on cycling and diff. LHCNM2 cells overexpressing HSPB2 showing HSPB2 and DAPI. IN, intranuclear.

(C) Immunofluorescence on HeLa cells overexpressing HSPB2 for 48 hr. Based on HSPB2 intranuclear distribution, cells were grouped into three categories: diffuse, foci, and compartments. The representative graph reports HSPB2 fluorescence intensity in each compartment normalized for the fluorescence intensity in the cytoplasm. n = 70–122. Data indicate mean ± SEM; $p < 10^{-26}$ (compartments versus diffuse HSPB2) and $p < 10^{-34}$ (foci versus diffuse HSPB2).

(D) Representative graphic showing HSPB2 critical threshold required for nuclear compartmentalization in diff. LHCNM2 cells. n = 100–111. Data indicate mean ± SEM; $p < 10^{-52}$ (foci versus diffuse HSPB2).

(E and F) Immunofluorescence on cycling and diff. LHCNM2 cells (E) or HeLa cells (F) overexpressing HSPB2. Staining: HSPB2 and LMNA.

(G) Immunofluorescence on diff. LHCNM2 cells showing nuclear foci containing endogenous HSPB2 and LMNA.

(H and I) Immunofluorescence on cycling and diff. LHCNM2 cells (H) or HeLa cells (I) overexpressing HSPB2. Staining: HSPB2 and prelamin-A.

In (A), (B), and (E)–(I), DAPI was used to stain nucleic acid. Scale bars, 10 μm.

See also Figures S1, S2, and S3.

To further investigate HSPB2 subcellular distribution, we overexpressed HSPB2 in cycling and differentiating LHCNM2 cells using lentiviral particles. By confocal microscopy, we confirmed that, similarly to endogenous HSPB2, overexpressed HSPB2 accumulated in the nucleus in cycling and differentiating LHCNM2 cells (Figure 1B). Again, we noticed heterogeneity in HSPB2 distribution. While some cells showed diffuse nuclear HSPB2 staining (Figure 1B, upper panel), others showed nuclear HSPB2 foci with variable size, ranging from 0.3 μm to 1.7 μm or more in diameter (Figure 1B, middle and lower panels; average size, 0.86 μm ± 0.02 μm; n = 167). Because HSPB3 is absent in cycling LHCNM2 cells, these findings suggest that overexpressed HSPB2 forms nuclear compartments in a HSPB3-independent manner. Moreover, HSPB2 assembly is independent of the developmental status of the cell, because we observed HSPB2 compartments in cycling and differentiating human myoblasts.

We then asked whether the formation of nuclear compartments by HSPB2 is specific to human myoblasts or whether it could also occur in other cell types. HSPB2 overexpressed in HeLa cells also showed a heterogeneous distribution: it was diffusely localized in the cytoplasm and nucleus, or enriched in nuclear foci of size ranging from ca. 0.4 μm to 3.8 μm in diameter (average size, 1.17 μm ± 0.03 μm; n = 169), or it accumulated in one large nuclear compartment (Figure 1C). Because MLO formation is dependent on protein concentration (Banani et al., 2017), we asked whether there is a critical concentration at which HSPB2 starts to form nuclear foci and larger compartments. Fluorescence density measurements allowed us to identify a critical threshold above which HSPB2 assembled into nuclear compartments (Figure 1C). We also identified a critical threshold at which endogenous HSPB2 formed nuclear compartments in differentiating human myoblasts (Figure 1D). The latter was similar to the one measured in HeLa cells overexpressing HSPB2. This result shows very clearly that compartmentalization by HSPB2 also occurs at endogenous expression levels and under physiological conditions.

Nuclear compartments of HSPB2 were also observed in immortalized motor neuronal (NSC34) and HEK293T cells (Figure S1D). Thus, HSPB2 compartmentalization is not cell type specific.

HSPB7 is also mainly expressed in myoblasts, similar to HSPB2 (Vos et al., 2009). In agreement with Vos et al. (2009), HSPB7 colocalized with the nuclear speckle marker ASF/SF2 in some HSPB7-overexpressing HeLa cells (data not shown). However, no nuclear compartments similar to the ones formed by HSPB2 were observed upon overexpression of HSPB7 in HeLa cells, even when a nuclear localization signal (NLS) was added to force HSPB7 nuclear accumulation (Figure S1E). HSPB1 and HSPB5, which translocate in the nucleus (Bryantsev et al., 2007; van den IJssel et al., 2003), did not form nuclear foci upon overexpression in HeLa cells either (Figure S1F). We conclude that compartment formation is a specific property of HSPB2, which is independent of the cell type but dependent on HSPB2 concentration.

HSPB2 Nuclear Compartments Sequester LMNA in Mammalian Cells

In LHCNM2 and HeLa cells, the large nuclear HSPB2 compartments affected chromatin distribution (judged by DAPI staining) and, occasionally, nuclear shape (Figures 1B and 1C). Nuclear shape and chromatin organization are regulated by nuclear lamins, which include LMNA, lamin-B1 (LMNB1), and B2 (LMNB2). These lamins form separate but interconnected meshwork underneath the nuclear envelope and throughout the nucleoplasm (Dechat et al., 2010). Thus, we asked whether HSPB2 nuclear compartments affected nuclear lamin distribution in myoblasts. Indeed, nuclear HSPB2 compartments colocalized with LMNA independent of their size; moreover, HSPB2 also changed LMNA distribution (Figure 1E). The changes in LMNA distribution induced by overexpressed HSPB2 also occurred in HeLa cells (Figure 1F).

We next verified whether the nuclear foci that HSPB2 forms during myoblast differentiation colocalize with LMNA. HSPB2 nuclear foci partly colocalized with LMNA (Figure 1G). These LMNA-positive HSPB2 foci were only observed in mononucleated cells that were in the process of differentiation. Thus, we conclude that HSPB2 forms intranuclear compartments in differentiating myoblasts, which sequester LMNA.

Mature LMNA originates from a precursor form, prelamin-A, which undergoes sequential post-translational modifications that include farnesylation and C terminus cleavage (Davies et al., 2011). Prelamin-A processing intermediates contribute to large-scale chromatin rearrangements, affecting the expression of specific genes. In particular, during myoblast differentiation, prelamin-A regulates the expression of key genes such as caveolin 3 and troponin T (Capanni et al., 2008). We asked whether HSPB2 nuclear compartments may also sequester immature forms of LMNA. Due to its rapid processing, prelamin-A is undetectable in mammalian cells unless its maturation is inhibited with, e.g., a specific farnesyltransferase inhibitor (FTI) (Verstraeten et al., 2008). In agreement, using an antibody specific for prelamin-A, we detected it only after treatment of cycling myoblasts with FTI (Figure S2A). Cycling and differentiating myoblasts overexpressing HSPB2 were characterized by the accumulation of prelamin-A in the form of nuclear foci that partly colocalized with HSPB2 compartments (Figure 1H). In contrast, prelamin-A was undetectable in cycling myoblasts overexpressing GFP (Figure S2B), excluding any artifact due to cell infection with lentiviral particles. Accumulation of prelamin-A inside HSPB2 nuclear compartments was also observed in HeLa cells (Figure 1I). The antibody used recognizes both non-farnesylated and farnesylated prelamin-A. To determine whether HSPB2 compartments equally recruit non-farnesylated and farnesylated prelamin-A, we co-expressed in HeLa cells HSPB2 with cDNAs expressing FLAG-prelamin-A (processed into mature lamin-A) and two mutants that cannot undergo complete maturation, FLAG-prelamin-A-C661M (non-farnesylatable) and FLAG-prelamin-A-L647R (uncleavable farnesylated) (Mattioli et al., 2011). HSPB2 compartments sequestered only FLAG-prelamin-A and non-farnesylated FLAG-prelamin-A-C661M, while leaving the distribution of farnesylated FLAG-prelamin-A-L647R unaffected (Figure S2C). Thus, HSPB2 sequesters immature non-farnesylated LMNA as well as mature LMNA in nuclear compartments and might interfere with LMNA maturation. Whether HSPB2-induced changes in prelamin-A and LMNA distribution have consequences on chromatin rearrangements and gene expression is unknown.

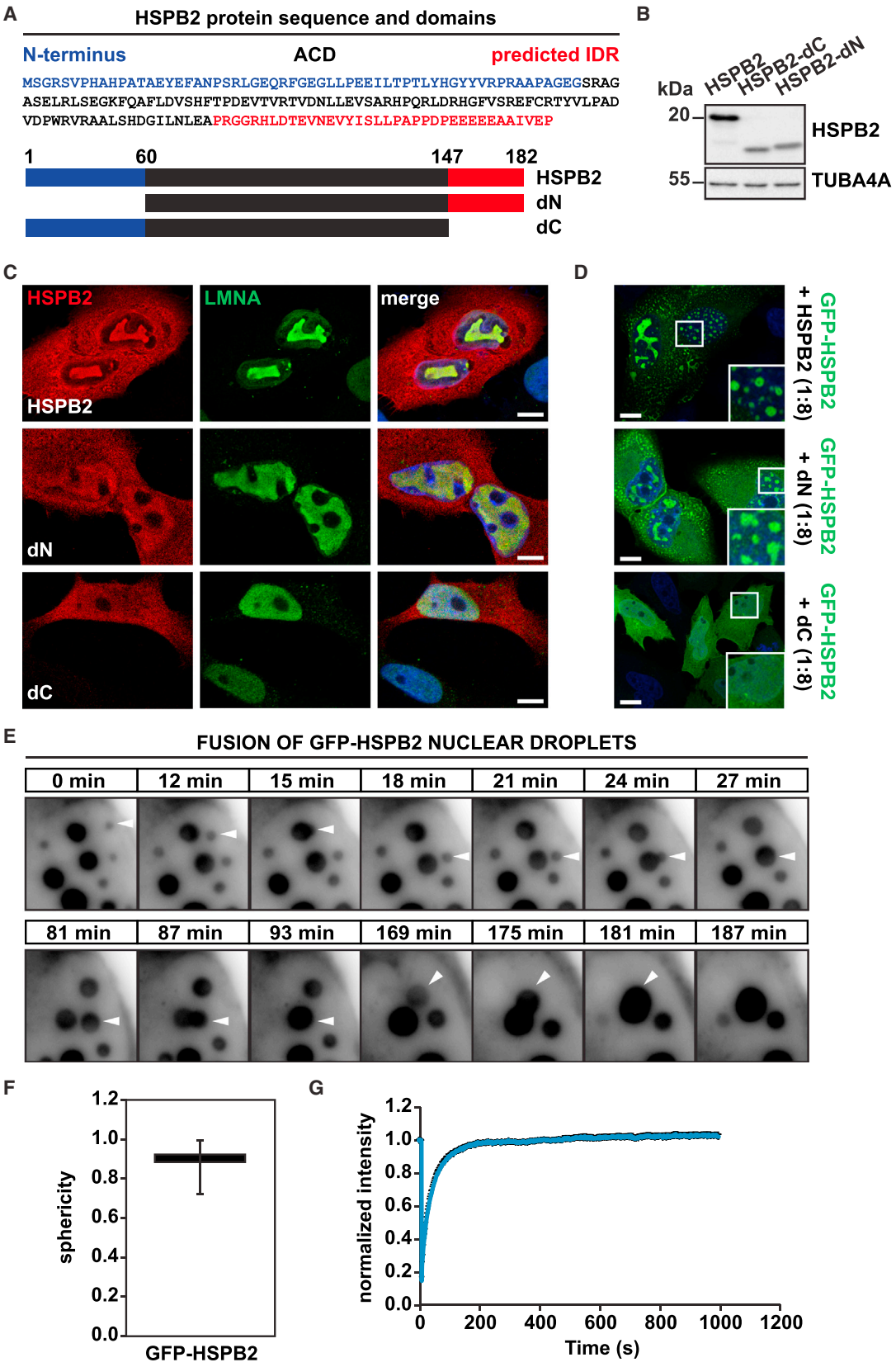

(legend on next page)

During differentiation, the solubility and distribution of LMNA change and these changes in the properties of LMNA are required for proper myoblast differentiation (Mariappan and Parnaik, 2005). Our data demonstrated that HSPB2 and LMNA colocalize in nuclear compartments during early myoblast differentiation and that overexpression of HSPB2 in LHCNM2 cells promotes targeting of nucleoplasmic LMNA, as well as non-farnesylated prelamin-A, to intranuclear compartments. We propose two possible explanations for these observations. First, HSPB2 forms compartments that directly sequester LMNA. Alternatively, LMNA itself could be enriched in nuclear compartments and then recruit HSPB2. To differentiate between these possibilities, we overexpressed HSPB2 in mouse embryonic fibroblasts (MEFs) derived from LMNA wild-type mice (*Lmna*$^{+/+}$), LMNA-deficient mice (*Lmna*$^{-/-}$), or mice that lack lamin A and express lamin-C only (LCO) (Figures S2D and S2E) (Lammerding et al., 2006). The absence of lamin-A (in LCO) and LMNA (in *Lmna*$^{-/-}$) did not abrogate HSPB2 assembly into compartments (Figure S2E). We conclude that HSPB2 forms intranuclear compartments independently of LMNA and that LMNA is recruited into HSPB2 compartments and not vice versa. Our results suggest a working model in which a local increase in HSPB2 concentration promotes HSPB2 compartmentalization, which, in turn, affects the intranuclear distribution of non-farnesylated prelamin-A and LMNA.

HSPB2 Compartments Behave as Liquid Droplets

HSPBs are disordered proteins because they contain N- and C-terminal IDRs (Sudnitsyna et al., 2012). However, the functional role of these IDRs is still unclear. Recent studies suggest that many IDRs promote the assembly of proteins into MLOs by liquid-liquid phase separation. The intranuclear assemblies formed by HSPB2 are reminiscent of MLOs. The fact that compartment formation by HSPB2 only occurs above a critical concentration (Figures 1C and 1D) is also typical for liquid-liquid phase separation (Banani et al., 2017; Schmidt and Rohatgi, 2016). Thus, we next tested whether the IDRs promote HSPB2 compartmentalization by phase separation.

We generated two truncated forms of HSPB2, lacking either the N terminus (dN-HSPB2) or the predicted disordered C-terminal domain (dC-HSPB2; Figure 2A). Both deletion mutants were expressed at similar levels in HeLa cells (Figure 2B). While HSPB2 and dN-HSPB2 still formed intranuclear compartments that sequestered LMNA, dC-HSPB2 showed a diffuse staining in the cytoplasm and nucleus and did not affect the distribution of LMNA (Figure 2C).

We next used live cell imaging with GFP-tagged HSPB2 to test whether HSPB2 compartments behave like liquid droplets. Because the GFP tag could influence the behavior of HSPB2, we overexpressed GFP-HSPB2 at a very low concentration, together with higher concentrations of untagged HSPB2, dN-HSPB2, or dC-HSPB2 (ratio of GFP-HSPB2:untagged HSPB2 constructs, 1:8). This strategy allowed us to recapitulate the previously observed subcellular distribution of untagged HSPB2 constructs (Figure 2; compare Figures 2C and 2D). Instead, GFP, per se, showed a homogeneous staining in HeLa cells (Movie S1). Upon co-transfection with full-length HSPB2 or dN-HSPB2, GFP-HSPB2 formed cytoplasmic and nuclear foci as well as large intranuclear assemblies (Figure 2D; Movies S2 and S3). However, GFP-HSPB2 displayed a diffuse distribution when co-expressed with dC-HSPB2 (Figure 2D; Movie S4).

We next characterized the behavior of GFP-HSPB2 compartments by live cell imaging. GFP-HSPB2 compartments have the typical properties of liquid droplets: they fuse after touching one another and then relax into one large droplet (Figure 2E; Movie S2), and they are roughly spherical, presumably due to the surface tension (Figure 2F). We next investigated the mobility of GFP-HSPB2 in the intranuclear compartments. Photobleaching analysis revealed that GFP-HSPB2 molecules rapidly redistribute within the nuclear assemblies, in agreement with a liquid material state (Figure 2G). Based on these data, we conclude that HSPB2 compartments have all the typical hallmarks of a liquid state, suggesting that HSPB2 compartments form via liquid-liquid phase separation.

We then verified whether HSPB2 compartments colocalize with known nuclear membrane-less organelles or recruit other IDR-containing proteins that undergo phase separation. The nuclear foci formed by overexpressed HSPB2 did not colocalize with nuclear speckles (SC35), Cajal bodies (SMN), nucleoli (fibrillarin), or nuclear stress bodies (Sam68) (Figure S3A). Adjacency and partial colocalization between some, but not all, HSPB2 foci and PML-nuclear bodies were observed. However, we also observed nuclear HSPB2 foci that were not adjacent to and did not colocalize with PML. Thus, HSPB2 nuclear foci can form independently of the presence of PML nuclear bodies (Figure S3A). Concerning RNA-binding proteins that undergo phase separation and are recruited to MLOs such as TIA-1, TDP-43 and FUS, these were not recruited at HSPB2 foci (Figure S3B).

Figure 2. The Intrinsically Disordered C-Terminal Domain of HSPB2 Is Required for Phase Separation in Cells

(A) Schematic representation of HSPB2 protein and of dN- and dC-HSPB2 deletion constructs generated. Blue indicates the N terminus; black indicates alpha-crystallin domain (ACD); red indicates predicted IDR.

(B) Immunoblot showing the expression levels of HSPB2, dC-HSPB2, and dN-HSPB2 in HeLa cells transfected for 48 hr. TUBA4A: loading control.

(C) Immunofluorescence on HeLa cells overexpressing HSPB2, dN-HSPB2, and dC-HSPB2.

(D) Microscopy on HeLa cells overexpressing GFP-HSPB2 with untagged HSPB2, dN-HSPB2, or dC-HSPB2 (1:8 ratio).

(E) Inverted black-and-white images of GFP-HSPB2 in HeLa cells overexpressing GFP-HSPB2 with HSPB2 (1:8 ratio). Fusion events of GFP-HSPB2 nuclear droplets are indicated by arrowheads.

(F) A boxplot showing the sphericity values of GFP-HSPB2 nuclear droplets (n = 72). Number 1 represents a sphere.

(G) Quantification of the fluorescence intensity recovery after bleach of GFP-HSPB2 nuclear droplets in HeLa cells overexpressing GFP-HSPB2 with HSPB2 (1:8 ratio). The timescale of a bleach experiment is shown. n = 18. Data indicate mean ± SEM.

Scale bars, 5 μm.

See also Figures S3 and S4 and Movies S1, S2, S3, and S4.

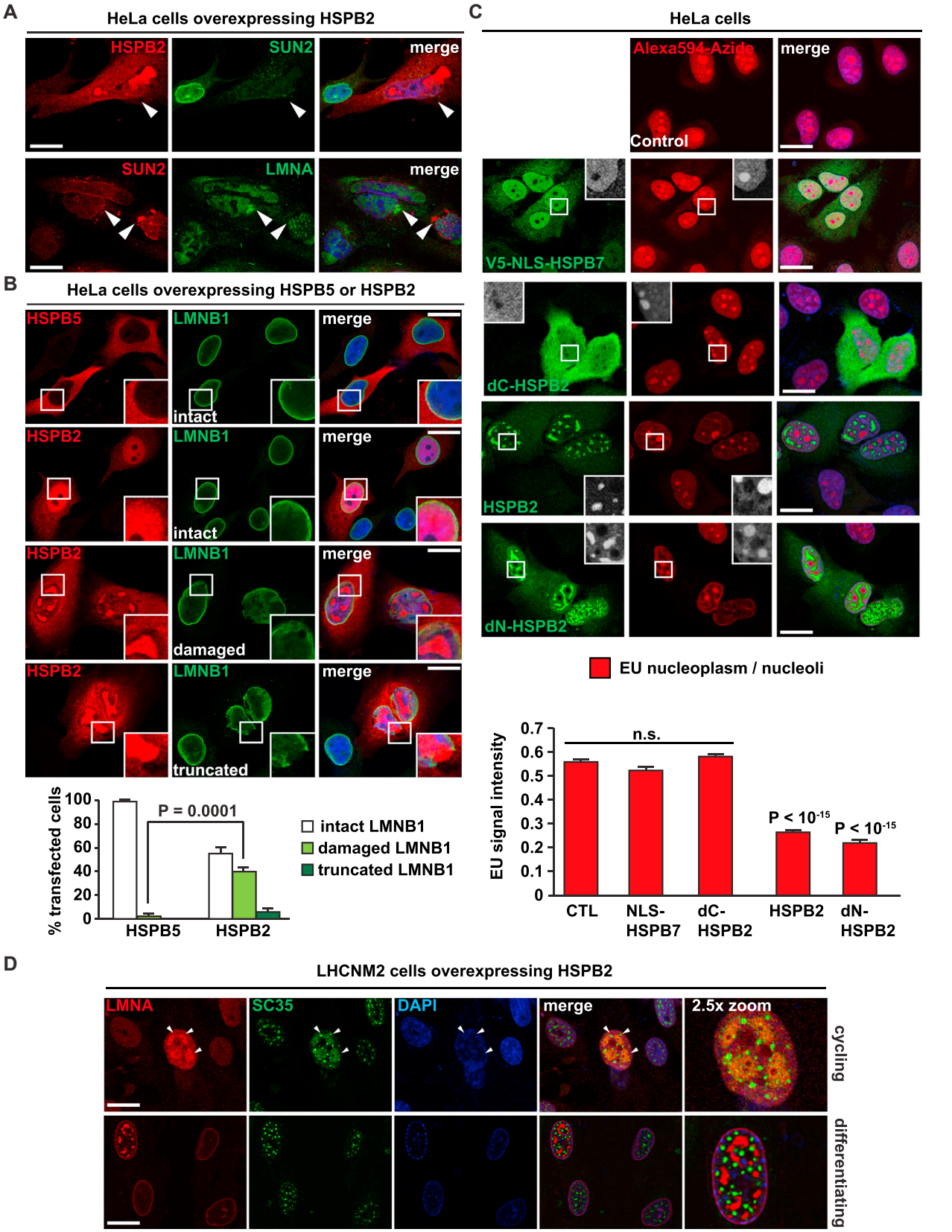

(legend on next page)

Combined, these results suggest that HSPB2 forms a type of MLO in mammalian cells.

HSPB2 Phase Separation Affects LMNA and Chromatin Distribution and Impairs Gene Transcription and Nuclear Integrity

To further study the functional consequences of HSPB2 phase separation, we performed live imaging and fluorescence recovery after photobleaching (FRAP) studies in cells co-expressing untagged HSPB2 and GFP-LMNA. Co-expression of untagged HSPB2, dN-HSPB2, or dC-HSPB2 with GFP-LMNA recapitulated the previously observed distribution of endogenous LMNA (compare Figure S4A with Figure 2C).

As expected, GFP-LMNA was almost completely immobile when expressed alone (Figure S4B; Movie S5), and the majority of GFP-LMNA was incorporated in the nuclear lamina (Gilchrist et al., 2004). In contrast, when co-expressed with HSPB2, a large fraction of GFP-LMNA formed dynamic droplets in the nucleoplasm (Movie S6). The pool of GFP-LMNA accumulating inside these nuclear droplets was highly mobile, as evidenced by FRAP measurements (Figure S4C) and droplet fusion events (Figure S4D). Instead, the pool of GFP-LMNA incorporated in the nuclear lamina was immobile, also upon co-expression of HSPB2 (data not shown). These results demonstrate that HSPB2 changes the intranuclear distribution and mobility of nucleoplasmic LMNA.

This result prompted us to investigate the localization of SUN2, an integral protein of the inner nuclear membrane (INM) whose anchoring to the nuclear envelope depends on LMNA (Liang et al., 2011). SUN2 was largely absent from the INM in cells with nuclear HSPB2 compartments (Figure 3A). This correlated with LMNA mislocalization and aggregation in the perinuclear region of the cell (Figure 3A, arrowheads). These results suggest that, by accumulating inside the nucleus, HSPB2 affects LMNA distribution and mobility, which, in turn, impairs SUN2 anchoring at the nuclear envelope, ultimately damaging its integrity. Consistently, HSPB2-overexpressing cells showed a significant increase in the percentage of cells with damaged or disrupted LMNB1 meshwork, compared to cells overexpressing HSPB5 (Figure 3B).

LMNA, together with nuclear-envelope-associated proteins, regulates DNA replication, chromatin organization, and gene transcription (Andrés and González, 2009). We studied whether HSPB2 compartments change chromatin distribution. We co-expressed GFP-HSPB2 in HeLa cells stably expressing histone H2B-mCherry and monitored the distribution of both proteins by time-lapse imaging. GFP-HSPB2 droplets displaced H2B-mCherry, changing chromatin distribution. These H2B-mCherry rearrangements were very dynamic because of the fusion events of GFP-HSPB2 droplets (Figure S4E; Movie S7). Displacement of H2B-mCherry and chromatin (judged by DAPI staining) by GFP-HSPB2 droplets was further confirmed by immunostaining on fixed cells (Figure S4F).

We then asked whether the changes in chromatin reorganization caused by HSPB2 phase separation could have functional consequences for gene transcription, which we measured using the uridine analog 5-ethynyl uridine (EU) (Jao and Salic, 2008). EU incorporation into newly synthesized RNA could be blocked by co-treatment of HeLa cells with actinomycin D, validating the experimental setup (Figure S5A). Overexpression of NLS-HSPB7, used as a negative control, did not affect EU incorporation, as compared to untreated HeLa cells (Figure 3C). In contrast, HSPB2 significantly decreased RNA synthesis (Figure 3C). Similar results were obtained in cycling myoblasts overexpressing GFP, used as control, or HSPB2. EU incorporation was not observed in areas that contained HSPB2 droplets, regardless of their small or larger size, and global RNA transcription in the nucleoplasm was reduced by HSPB2 phase separation (Figure S5B).

Next, we studied whether HSPB2 compartments would also impair RNA transcription in LMNA knockout cells. Similarly to what is observed in HeLa and LHCNM2 cells, HSPB2 compartments locally inhibited EU incorporation in LMNA-proficient MEFs (Figure S5C). In contrast, in LMNA knockout MEFs, EU was still efficiently incorporated into HSPB2 compartments (Figure S5C). This result demonstrates that HSPB2 compartmentalization leads to a spatial rearrangement of lamin-A and locally impairs RNA synthesis.

Another indirect measure of RNA transcription is reflected by the change in the shape of nuclear speckles. Speckles are dynamic MLOs that store splicing factors (Lamond and Spector, 2003). While, in resting cells, speckles have an irregular shape, they reorganize into spherical foci when polymerase-II-mediated transcription is blocked with actinomycin D (Lamond and Spector, 2003). Moreover, changes in the levels and distribution of LMNA inhibit polymerase II-mediated transcription, with consequences on speckle shape (Shimi et al., 2008; Spann et al., 2002). These findings open the possibility that HSPB2 phase separation, by changing LMNA and chromatin distribution, may also indirectly lead to the reorganization of speckles into spherical foci. To verify this hypothesis, we overexpressed HSPB2 in myoblasts, and we studied the subcellular distribution of LMNA and SC35, a speckle marker. Speckles had an irregular shape in myoblasts with diffuse LMNA distribution

Figure 3. HSPB2 Aberrant Phase Separation Inhibits RNA Synthesis

(A) Immunofluorescence on HeLa cells overexpressing HSPB2 showing SUN2 recruitment at the nuclear envelope.

(B) Immunofluorescence on HeLa cells overexpressing HSPB5 or HSPB2. Damaged LMNB1: irregular and discontinuous nuclear rim; truncated LMNB1: nuclear rim missing one or more portions in the proximity of HSPB2 compartments. Data indicate mean ± SEM.

(C) 40 hr post-transfection, HeLa cells, control or overexpressing V5-NLS-HSPB7 or HSPB2, were incubated with 5-ethynyl uridine (EU; 200 μM) for 6 hr. Staining: Alexa594-Azide, V5, HSPB2, and DAPI. EU intensity was quantified in nucleoli and nucleoplasm; nucleoplasm/nucleoli ratio was calculated. n = 30–36. Data indicate mean ± SEM; $p < 10^{-15}$. n.s., not significant.

(D) Cycling and differentiating (diff.) LHCNM2 cells overexpressing HSPB2 were stained for LMNA, SC35, and DAPI.

Scale bars, 10 μm.

See also Figures S4 and S5 and Movies S5, S6, and S7.

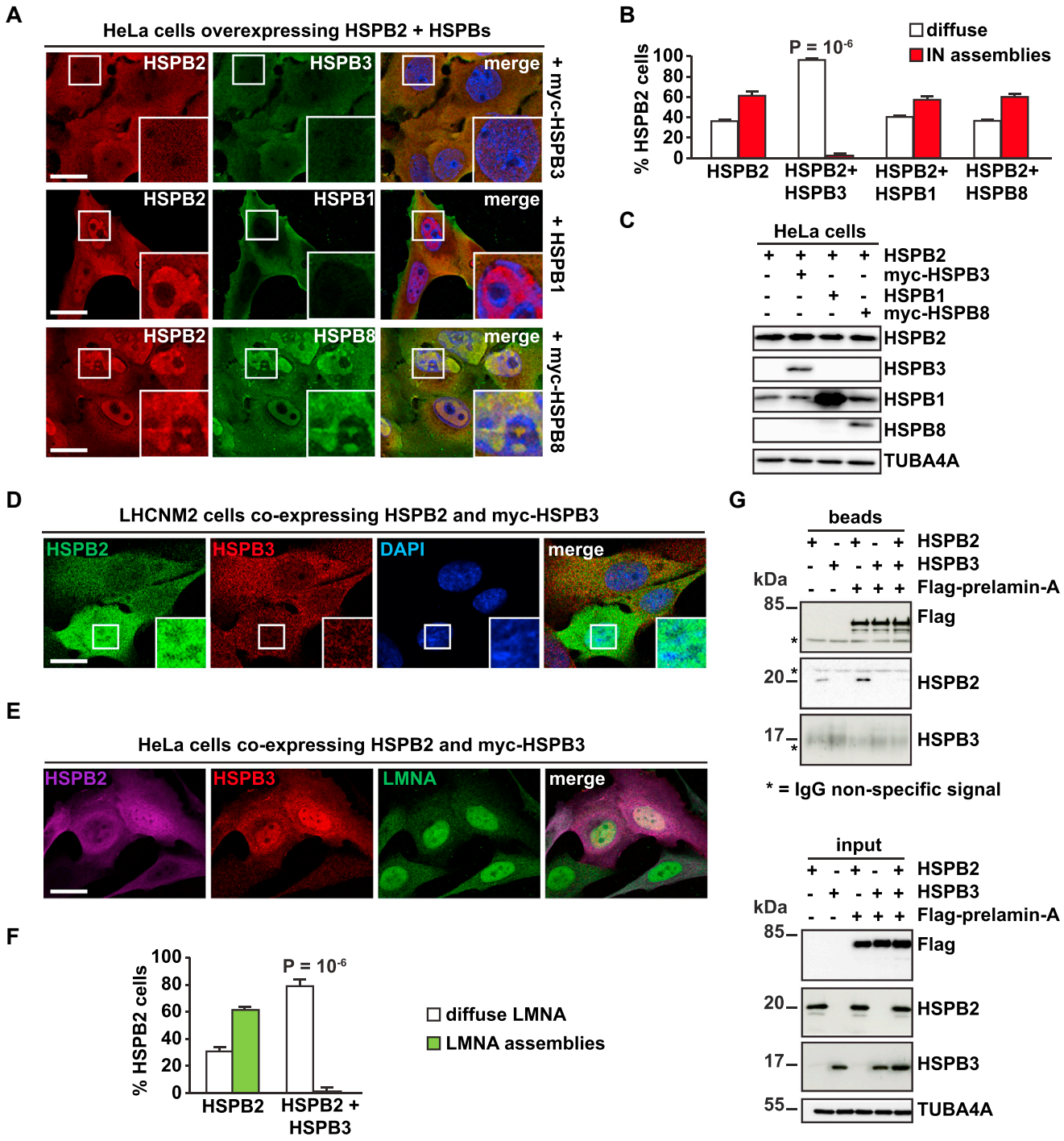

Figure 4. HSPB3 Inhibits HSPB2 Aberrant Phase Separation

(A) Immunofluorescence on HeLa cells overexpressing HSPB2 with myc-HSPB3, HSPB1, or myc-HSPB8.

(B) Quantitation of the percentage of HSPB2-overexpressing cells with diffuse staining or HSPB2 nuclear assemblies. n = 3 experiments/conditions. Data indicate mean ± SEM; $p = 4.17 \times 10^{-6}$. 143–180 cells per experiment were analyzed.

(C) Immunoblot showing levels of HSPB2, HSPB1, myc-HSPB3, and myc-HSPB8 in transfected HeLa cells. TUBA4A: loading control.

(D) Immunofluorescence on cycling myoblasts overexpressing HSPB2 and HSPB3. One representative image of 478 cells analyzed, all showing diffuse HSPB2.

(E) Immunofluorescence on HeLa cells overexpressing HSPB2 with myc-HSPB3 showing endogenous LMNA.

(F) Microscopy on HeLa cells overexpressing HSPB2 alone or with myc-HSPB3. Quantitation of the percentage of cells with LMNA nuclear compartments is shown. n = 3–4 experiments/conditions. Data indicate mean ± SEM; $p = 3.72 \times 10^{-6}$. 125–200 cells per experiment were analyzed.

(legend continued on next page)

and a spherical shape in myoblasts where LMNA was sequestered into HSPB2 compartments (Figure 3D). These data further support the interpretation that HSPB2 phase separation, by altering LMNA and chromatin distribution, inhibits RNA transcription.

Based on these results, we define the nuclear droplets formed in differentiating human myoblasts as "physiological" HSPB2 compartments. In contrast, we refer to HSPB2 droplets that form upon transient overexpression as "aberrant" HSPB2 compartments because they mislocalize LMNA and chromatin, with detrimental consequences for nuclear integrity and function.

HSPB3 Inhibits Aberrant Compartment Formation by HSPB2 and Restores Nuclear LMNA Distribution

HSPB2 forms a stoichiometric complex with HSPB3 (3:1), and their interaction co-stabilizes both proteins (den Engelsman et al., 2009). Physiological intranuclear HSPB2 compartments that form in differentiating myoblasts did not colocalize with HSPB3 but partly colocalized with LMNA (Figure 1G). However, the cytoplasmic HSPB2 foci partly colocalized with HSPB3 (Figure S1C). We thus asked whether HSPB3 could influence HSPB2 phase separation. We co-transfected HSPB2 and HSPB3 in HeLa cells and compared the propensity of HSPB2 to form intranuclear assemblies in the presence and absence of HSPB3. HSPB3 prevented the formation of nuclear HSPB2 droplets, because both proteins were homogeneously distributed throughout the cells (Figures 4A and 4B). This effect was not a mere consequence of lower HSPB2 expression levels upon its co-transfection with HSPB3, as confirmed by immunoblotting (Figure 4C; see also Figure 5G). In contrast, co-expression with HSPB1 or HSPB8 did not prevent HSPB2 compartmentalization (Figures 4A and 4B). While HSPB8 was sequestered inside HSPB2 nuclear compartments, HSPB1 was not (Figure 4A). This result suggests some additional specificity in sequestering proteins in HSPB2 compartments. Also, in cycling LHCNM2 cells co-expressing HSPB3 and HSPB2, the latter showed a homogeneous distribution (Figure 4D), further confirming that HSPB3 negatively regulates HSPB2 compartmentalization.

Since LMNA distribution is rearranged due to HSPB2 aberrant phase separation, we tested whether co-expression of HSPB2 with HSPB3 could rescue LMNA distribution. Indeed, overexpression of HSPB3 inhibited HSPB2 aberrant phase separation and maintained proper LMNA distribution (Figures 4E and 4F). These results demonstrate that nuclear phase separation is a specific property of HSPB2 that is negatively regulated by HSPB3.

We next asked whether HSPB2 directly binds to LMNA and whether/how HSPB3 affects HSPB2-LMNA association. We overexpressed FLAG-tagged LMNA with HSPB2 and HSPB3, separately or combined. Co-immunoprecipitation studies revealed that HSPB2, but not HSPB3, weakly binds to LMNA (Figure 4G). When co-expressed with HSPB2, HSPB3 abolished the association between HSPB2 and LMNA (Figure 4G). These results support the interpretation that, by directly binding to HSPB2, HSPB3 prevents both HSPB2 compartmentalization and association with LMNA.

Identification of Two Putative *HSPB3* Mutations in Myopathy Patients

Mutations in the *HSPB1*, *HSPB5*, and *HSPB8* genes cause myopathy and/or neuropathy (Boncoraglio et al., 2012). Recently, the missense variant p.R7S (rs139382018) in *HSPB3* was linked to axonal motor neuropathy (HMN2C). However, the underlying mechanism is yet unknown (Kolb et al., 2010). Because of the high expression of HSPB2 and HSPB3 in skeletal muscles (Sugiyama et al., 2000), we hypothesized that mutations in this complex could cause (neuro)muscular diseases. Therefore, we sequenced the genomic DNA of 400 myopathy patients of unknown origin to identify potential mutations in the coding regions of *HSPB2* and *HSPB3*. We identified two variants in *HSPB3* in two independent cases that included the A33AfsX50-HSPB3 truncation variant and the R116P-HSPB3 rare missense variant (rs150931007), with a minor allele frequency of 0.0001730 in the ExAC browser (assessed March 2017) (Figures 5A and S6A–S6C). Unfortunately, we were unable to test the parents of case 1 (Figure S6A); the father of case 2 (Figure S6B), who also carried the R116P-HSPB3 variant, displayed only moderate symptoms at the time of testing. The R116P-HSPB3 variant affects a highly conserved, key amino acid in the α-crystallin domain of HSPB3 (Figure S6C), whereas the A33AfsX50-HSPB3 mutation disrupts the reading frame at alanine 33, leading to a premature stop codon 50 amino acids later. This event very likely leads to a non-functional protein.

The A33AfsX50-HSPB3 mutation was found in a 70-year-old Italian man who presented shoulder-girdle muscle weakness and atrophy. The R116P-HSPB3 mutation was found in a 25-year-old woman of Italian origin. The father of the affected patient, carrier of the R116P-HSPB3 mutation, was pauci-symptomatic and presented sciatic irregular pains, similar to his daughter with intermittent myalgia. By the age of 32 years, the affected patient developed weakness of the upper and lower limbs, along with neurogenic changes in the lower limbs compatible with axonal neuropathy. Electron microscopy of her muscle biopsy showed severe myofibrillar disarray with loss of Z-disk, enlargements of sarcoplasmic reticulum cisternae, few lysosomes, and sub-sarcolemmal and intermyofibrillar glycogen accumulations in several fibers (Figure 5B). Importantly, the nuclei were plurisegmented with marginated chromatin (Figures 5C and 5D), a hallmark reminiscent of cells overexpressing HSPB2.

These two cases join the growing list of disease-causing mutations reported in HSPB genes.

R116P-HSPB3 and A33AfsX50-HSPB3 Disrupt HSPB2-HSPB3 Complex Formation and Cannot Regulate HSPB2 Aberrant Phase Separation

To study whether the two newly identified mutations affect HSPB3 expression and interaction with HSPB2, we overexpressed

(G) Immunoprecipitation with anti-FLAG of HEK293T cells overexpressing for 24 hr FLAG-prelamin-A and an empty vector or HSPB2 alone or with myc-HSPB3. Total cell lysates (input) and immunocomplexes (beads) were processed for western blot. Asterisk indicates immunoglobulin G (IgG) or non-specific signal.
Scale bars, 10 μm.
See also Figure S6.

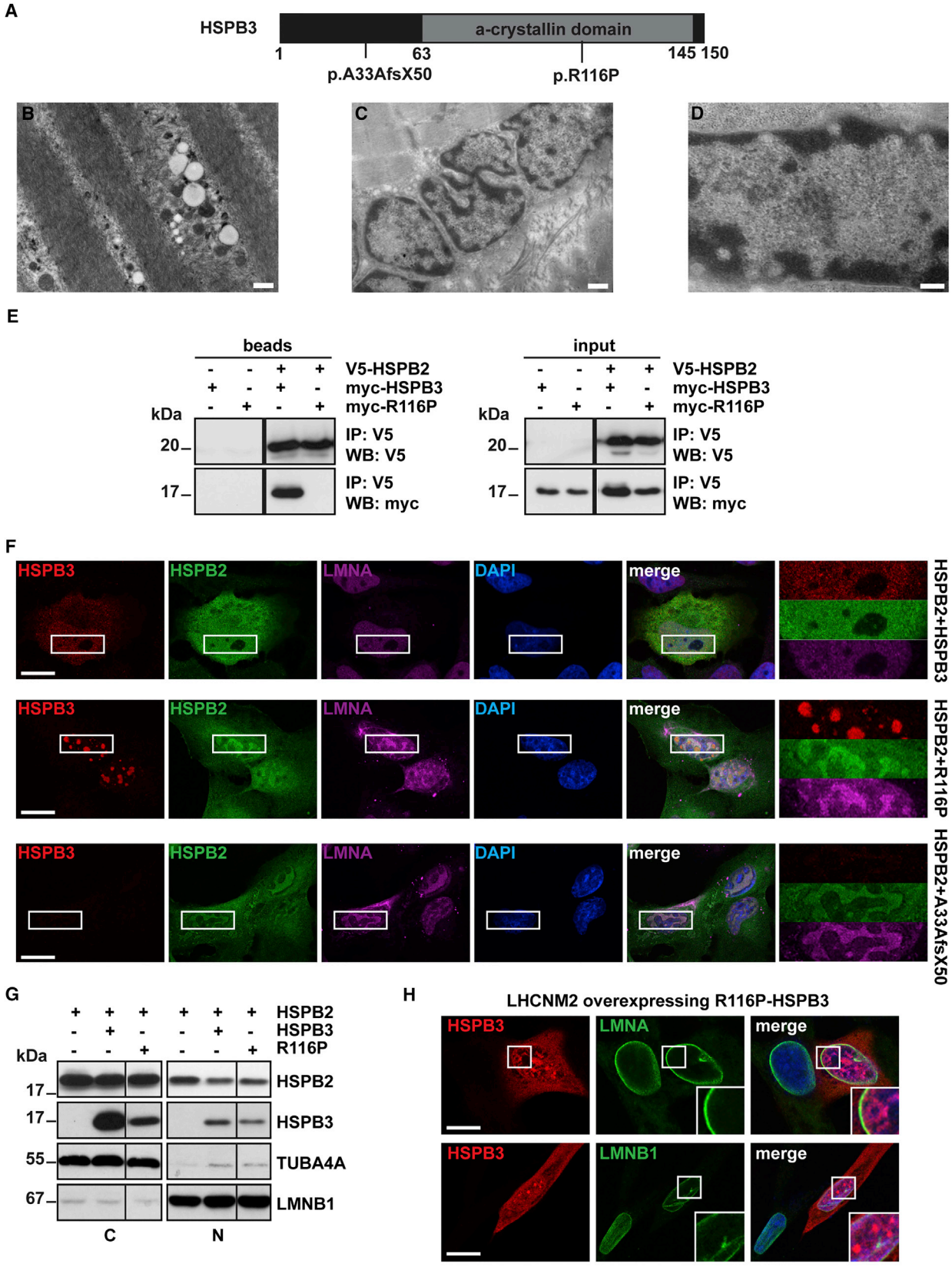

(legend on next page)

myc-tagged HSPB3, R116P-HSPB3, and A33AfsX50-HSPB3 in HeLa cells and measured HSPB3 mRNA and protein levels. The mRNA levels of both mutants were higher compared to those of HSPB3 (Figure S6D). However, the R116P-HSPB3 protein was expressed at similar levels compared to HSPB3, whereas A33AfsX50-HSPB3 was undetectable. This suggested that A33AfsX50-HSPB3 is rapidly degraded after synthesis. This hypothesis was tested and confirmed using Bortezomib, a proteasome inhibitor (Figure S6E).

Next, we verified by co-immunoprecipitation whether the R116P mutation affects HSPB3 binding to HSPB2. While the wild-type proteins interacted (den Engelsman et al., 2009), no association was detected between HSPB2 and R116P-HSPB3 (Figure 5E). A33AfsX50-HSPB3 levels were barely detectable; therefore, its binding to HSPB2 was not tested. Thus, the two mutations identified in myopathy patients directly (R116P) or indirectly (A33AfsX50) disrupt the formation of the HSPB2-HSPB3 complex.

In light of these results, we then tested whether A33AfsX50-HSPB3 and R116P-HSPB3 can inhibit HSPB2 aberrant phase separation. Neither A33AfsX50-HSPB3 nor R116P-HSPB3 could inhibit the formation of HSPB2 nuclear droplets (Figure 5F). Intriguingly, R116P-HSPB3 formed intranuclear aggregates, which were often adjacent but excluded from HSPB2 droplets (Figure 5F). Importantly, in cells co-expressing R116P-HSPB3 or A33AfsX50-HSPB3 together with HSPB2, LMNA was sequestered into HSPB2 nuclear droplets. The nuclear amount of HSPB2 was similar in HeLa cells co-expressing HSPB2 with HSPB3 or R116P-HSPB3; however, HSPB2 formed compartments that sequestered LMNA only in cells co-expressing R116P-HSPB3 (Figure 5G). In agreement, LMNA could still co-immunoprecipitate HSPB2 in cells co-expressing R116P-HSPB3; as an additional control, the neuropathy-linked R7S mutant of HSPB3, which still binds to HSPB2 as efficiently as wild-type HSPB3, abrogated the HSPB2-LMNA interaction (Figures S6F and S6G). These results demonstrate that both HSPB3 mutants cannot negatively regulate HSPB2 aberrant phase separation.

Formation of nuclear aggregates by R116P-HSPB3 was confirmed using cycling myoblasts. Similarly to what was observed in HeLa cells, R116P-HSPB3 nuclear aggregates did not colocalize with LMNA and LMNB1 (Figure 5H). Since cycling myoblasts do not express endogenous HSPB2, these results demonstrate that formation of nuclear aggregates is an intrinsic property of R116P-HSPB3.

Depletion of HSPB3 Enhances HSPB2 Compartmentalization and Leads to Nuclear Morphological Defects

We demonstrated that HSPB3 disease-linked mutants inhibit the formation of the HSPB2-HSPB3 complex. This result opens the possibility that the accumulation of a free pool of HSPB2, which can self-assemble, might affect gene expression and nuclei morphology, thereby contributing to HSPB3-linked disease. To address this hypothesis, we silenced HSPB3 in differentiating myoblasts. LHCNM2 cells were infected with lentiviral particles expressing a non-targeting short hairpin RNA (shRNA) control sequence or a specific HSPB3 shRNA sequence and GFP as reporter. Five days post-differentiation, cells were processed for qPCR, immunoblotting, or immunohistochemistry. HSPB3 depletion was efficient and did not affect the expression of HSPB2, compared to control cells (Figures 6A and 6B). HSPB3 depletion significantly decreased the expression of myogenin, one of the key genes required for myoblast differentiation (Figure 6A). Concerning the subcellular distribution of HSPB2, 5 days post-differentiation, it was mainly homogeneous in control differentiating cells, with few nuclear HSPB2-positive foci detectable in ca. 34% of the infected cells. In contrast, more than 67% of HSPB3-depleted cells were characterized by the presence of HSPB2-positive foci in the nucleus and cytoplasm (Figure 6C). Besides, compared to control cells, HSPB3-depleted cells were characterized by nuclear morphology abnormalities, with a significant increase of micronuclei (Figures 6D and 6E). These data support the idea that imbalances in the expression of HSPB2-HSPB3 and accumulation of a free pool of HSPB2 correlate with nuclear alterations and impaired myogenin expression.

DISCUSSION

Phase separation of IDR-containing proteins drives the assembly of intracellular components into MLOs that behave like liquid droplets and exert specific functions. The most extensively studied MLOs are cytoplasmic stress granules, P bodies, nuclear speckles, Cajal bodies, and nucleoli (Banani et al., 2017). Recently, phase separation has also been implicated in the

Figure 5. Two HSPB3 Myopathy Mutants Cannot Inhibit HSPB2 Aberrant Phase Separation

(A) Schematic representation of HSPB3 protein structure and position of the two HSPB3 mutations identified in myopathy patients (p.A33AfsX50 and p.R116P).

(B–D) Electron microscopy on the muscle biopsy of the 25-year-old patient carrying the R116P mutation of HSPB3.

(B) Scale bar, 5 μm.

(C and D) Scale bars, 0.1 μm.

(C) Nuclear deformation and chromatin margination.

(D) Chromatin margination.

(E) Immunoprecipitation with anti-V5 on cells overexpressing for 24 hr V5-tagged HSPB2 and myc-tagged HSPB3 or R116P-HSPB3. Input and immunocomplexes (beads) were processed for immunoblotting. WB, western blot.

(F) Immunofluorescence on HeLa cells overexpressing HSPB2 with myc-tagged HSPB3, R116P-HSPB3, or A33AfsX50-HSPB3 showing HSPB2, HSPB3, LMNA, and nucleic acid (DAPI).

(G) Nucleus/cytoplasm fractionation of HeLa cells overexpressing HSPB2 alone or with myc-tagged HSPB3 or R116P-HSPB3.

(H) Immunofluorescence on cycling myoblasts overexpressing R116P-HSPB3 and stained for HSPB3 and LMNA or LMNB1.

Scale bars, 10 μm.

See also Figure S6.

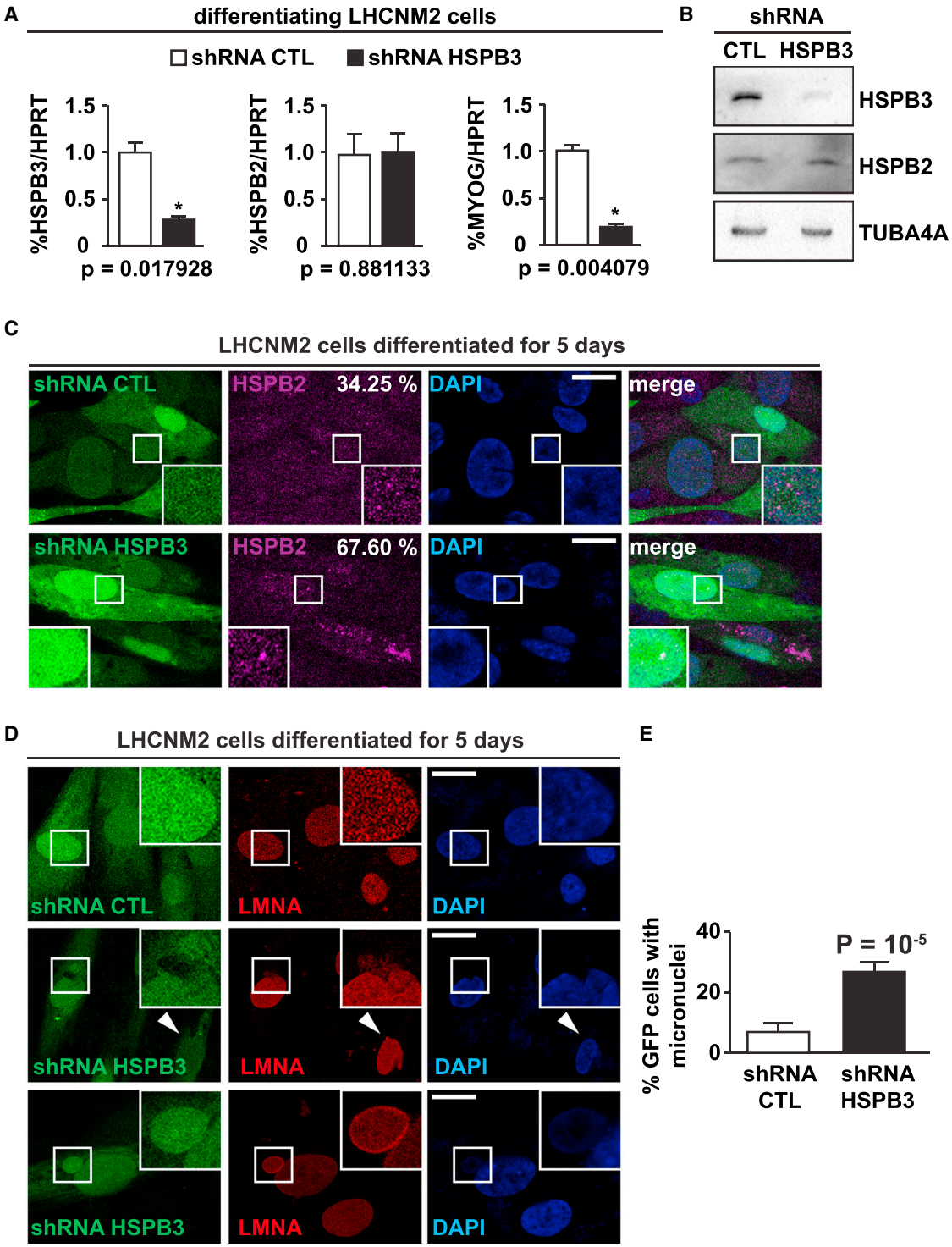

Figure 6. Depletion of HSPB3 Increases HSPB2 Compartmentalization, Decreases Myogenin Expression, and Affects Nuclear Morphology

(A) mRNA levels of HSPB3, HSPB2, and myogenin in LHCNM2 cells infected with non-targeting shRNA (CTL) or HSPB3 shRNA and differentiated for 5 days. HPRT was used for normalization.

(B) Protein levels of HSPB2, HSPB3, and TUBA4A (loading control) in samples treated as described in (A).

(C) Cells were treated as described in (A) and processed for immunofluorescence using the HSPB2 antibody. The percentage of cells with HSPB2-positive foci is shown (181 cells expressing shRNA CTL and 179 cells expressing shRNA HSPB3 were analyzed).

(D) Microscopy on LHCNM2 cells infected as described in (A), showing LMNA distribution and nuclear morphology (DAPI).

(legend continued on next page)

DNA damage response (Aguzzi and Altmeyer, 2016). Poly(ADP-ribose) (PAR) nucleates liquid demixing of IDR-containing proteins at sites of DNA damage. PAR-seeded liquid demixing enables the dynamic rearrangement of nuclear architecture, concentrating and organizing the players that orchestrate DNA repair (Aguzzi and Altmeyer, 2016). Phase separation is, thus, emerging as an efficient mechanism by which cells control the spatio-temporal localization and mobility of specific macromolecules, and regulate complex cellular functions.

Myoblast differentiation is characterized by changes in nuclear architecture, reorganization of nuclear LMNA, and a transient increase in targeted DNA strand breaks, which enhances muscle gene expression (Fernando et al., 2002; Larsen et al., 2010; Markiewicz et al., 2005). DNA damage is followed by caspase-triggered XRCC1 repair foci; the latter allows proceeding along muscle differentiation (Al-Khalaf et al., 2016). Interestingly, LMNA promotes DNA repair, stabilizing 53BP1 and preventing DNA damage and cell senescence (Gonzalez-Suarez et al., 2009; Lees-Miller, 2006). Moreover, LMNA remodeling is required for proper gene expression during myoblast differentiation (Markiewicz et al., 2005), and overexpression of LMNA upregulates muscle-specific genes (Lourim and Lin, 1992). Thus, changes in LMNA concentration and distribution directly affect chromatin and gene expression, and LMNA remodeling and DNA repair are interconnected processes, at least during myoblast differentiation.

Our study shows that HSPB2 forms liquid compartments that partly colocalize with LMNA in differentiating myoblasts. This suggests that HSPB2 compartments regulate nucleoplasmic LMNA rearrangements that take place during the early steps of muscle differentiation. Phase-separated HSPB2 may temporarily store discrete pools of LMNA, delaying their incorporation in the nuclear envelope (Markiewicz et al., 2005). Recruitment of LMNA into nuclear HSPB2 storage compartments could drive subtle changes in chromatin organization, influencing transcription of specific genes. In line, LMNA remodeling due to HSPB2 phase separation leads to a redistribution of chromatin, with direct consequences for nuclear transcription.

Muscles are subjected to oxidative and mechanical stress. LMNA remodeling activates the transcription of genes required in response to mechanical stress, a process known as mechanotransduction (Lammerding et al., 2006). HSPB2 may regulate specific LMNA rearrangements, indirectly regulating chromatin organization in mechanically stressed cells. Accordingly, upon exposure to oxidative stress, *HSPB2* knockout mice fail to properly modulate the transcription of metabolic and mitochondrial regulatory genes required for the stress response; this, in turn, has detrimental consequences for muscle viability (Ishiwata et al., 2012). Moreover, *HSPB2*/*HSPB5* double-knockout mice develop myopathy with aging, supporting the conclusion that HSPB2 (with HSPB5) is required for myoblast adaptation and response to chronic stress.

An increasing body of evidence shows that deregulated phase separation has strong implications in aging and disease, including, e.g., amyotrophic lateral sclerosis and inclusion body myopathy (Aguzzi and Altmeyer, 2016; Alberti and Hyman, 2016). Here, we provide further evidence that derailed phase separation can be a determinant of cellular dysfunction and human disease. First, deregulated HSPB2 phase separation mislocalizes LMNA, compromising nuclear architecture and transcription; however, aberrant compartmentalization by HSPB2 is counteracted by HSPB3, which is co-upregulated with HSPB2 during myoblast differentiation (Sugiyama et al., 2000). Intriguingly, HSPB3 depletion in differentiating myoblasts decreases myogenin expression and enhances HSPB2 compartmentalization and nuclear morphological defects such as micronucleus accumulation. These observations suggest that imbalances of HSPB2-HSPB3 expression and enhanced HSPB2 foci formation may have deleterious consequences on myoblast viability and differentiation. Second, we identified two HSPB3 mutations in myopathy patients. While A33AfsX50-HSPB3 is unstable and rapidly degraded, R116P-HSPB3 can no longer interact with HSPB2. Thus, both HSPB3 mutants cannot control HSPB2 aberrant phase separation. Intriguingly, a muscle biopsy from the patient with the R116P-HSPB3 mutation shows alterations of nuclear morphology with chromatin margination. Although we do not know whether aberrant HSPB2 compartmentalization occurred in patient cells, these changes are similar to the ones induced by HSPB2 overexpression. Concerning R116P-HSPB3-linked myopathy, we cannot exclude that R116P-HSPB3 is associated with a gain of toxic function, as suggested by its propensity to form nuclear aggregates. It is possible that both a gain of toxic function of HSPB3 and a loss of function resulting from deregulated HSPB2 phase separation and LMNA mobility contribute to disease.

In line, increased retention of LMNA in the nucleoplasm, increased LMNA mobility and solubility, and accumulation of micronuclei have been documented in mammalian and patient cells expressing mutated forms of LMNA associated with laminopathies (Gilchrist et al., 2004; Markiewicz et al., 2002, 2005). Laminopathies include a variety of human diseases, such as Emery-Dreifuss muscular dystrophy, dilated cardiomyopathy, and Hutchinson-Gilford progeria syndrome, that are characterized by muscle atrophy, together with other symptoms (Davidson and Lammerding, 2014). Moreover, loss of LMNA disrupts nuclear envelope integrity and causes muscular dystrophy in mice (Sullivan et al., 1999). Altogether, these data highlight the importance of LMNA for muscle cell function and how aberrant changes in its distribution are detrimental for muscle viability.

In summary, we propose that HSPB2 phase separation regulates dynamic LMNA and chromatin remodeling in response to differentiation stimuli and upon stress, maintaining myoblast viability. In contrast, deregulation of HSPB2 compartmentalization, due to decreased HSPB3 expression or HSPB3 mutations

(E) Cells were treated as described in (A). Quantitation of the percentage of cells with micronuclei. n = 8. Data indicate mean ± SEM; $p = 1.23 \times 10^{-5}$ (423 cells expressing shRNA CTL and 390 cells expressing shRNA HSPB3 were analyzed).
Scale bars, 10 μm.
See also Figure S6.

that disrupt the HSPB2-HSPB3 complex, may contribute to muscle aging and disease.

EXPERIMENTAL PROCEDURES

Cell Lines

In this study we used: LHCNM2 human myoblasts; HeLa, NSC34, and HEK293T cells; Lmna$^{+/+}$, Lmna$^{-/-}$, and LCO mouse embryonic fibroblasts; and HeLa-Kyoto cells expressing mCherry-tagged human H2B.

Collection of Human Samples

Procedures for collection of human blood and muscle biopsy were in accordance with the ethical standards of the regional committee (approval received on 09/10/2007). Informed consent was obtained from all subjects. At the time of muscle biopsy, the proband was a 25-year-old woman. When she was re-evaluated at 32 years of age, the proband showed a mild proximal and distal muscle weakness. Muscle biopsy was done at the left deltoid. Muscle was flash frozen in isopentane cooled in liquid nitrogen and stored at −80 degrees until analysis.

Statistical Analysis

Student's t test was used for comparisons between two groups. One-way ANOVA followed by a Bonferroni-Holm post hoc test was used for comparisons between three or more groups.

SUPPLEMENTAL INFORMATION

Supplemental Information includes Supplemental Experimental Procedures, six figures and seven movies and can be found with this article online at http://dx.doi.org/10.1016/j.celrep.2017.08.018.

AUTHOR CONTRIBUTIONS

Conceptualization, F.F.M. and S.C.; Methodology, F.F.M., J.B., and S.C.; Formal Analysis, F.F.M., J.B., J.V., and S.C.; Investigation, F.F.M., J.B., D.S.V., J.V., G.C., L.M., S.D.B., M.N., and S.C.; Resources, S.M., J.L., J.F.B., R.T., E.P., and C.A.; Writing – Original Draft, F.F.M. and S.C.; Writing – Review & Editing, S.A. and S.C.; Supervision, S.A. and S.C.; Funding Acquisition, S.C.

ACKNOWLEDGMENTS

We thank Dr. L. Heldens, Dr. G. Leo, Dr. C. Imbriano, CIGS, and people from the MPI-CBG microscopy facility for technical support. We thank Dr. T.M. Franzmann and Dr. S. Maharana for help with data analysis. We thank Telethon Genetic BioBank (GTB12001D to E.P.) and Eurobiobank Network for the muscle biopsy and Dr. W. Boelens and Dr. I. Benjamin for fruitful discussion. S.C. thanks Telethon (GEP12008 and GGP15001) and Association Française contres les Myopathies (15999) for financial support. S.A. acknowledges funding from the Max Planck Society, and J.L. acknowledges funding from NIH (R01 HL082792) and BCRP (BC150580).

Received: April 4, 2017
Revised: July 10, 2017
Accepted: August 1, 2017
Published: August 29, 2017

REFERENCES

Aguzzi, A., and Altmeyer, M. (2016). Phase separation: linking cellular compartmentalization to disease. Trends Cell Biol. *26*, 547–558.

Al-Khalaf, M.H., Blake, L.E., Larsen, B.D., Bell, R.A., Brunette, S., Parks, R.J., Rudnicki, M.A., McKinnon, P.J., Dilworth, F.J., and Megeney, L.A. (2016). Temporal activation of XRCC1-mediated DNA repair is essential for muscle differentiation. Cell Discov. *2*, 15041.

Alberti, S., and Hyman, A.A. (2016). Are aberrant phase transitions a driver of cellular aging? BioEssays *38*, 959–968.

Andrés, V., and González, J.M. (2009). Role of A-type lamins in signaling, transcription, and chromatin organization. J. Cell Biol. *187*, 945–957.

Andrés, V., and Walsh, K. (1996). Myogenin expression, cell cycle withdrawal, and phenotypic differentiation are temporally separable events that precede cell fusion upon myogenesis. J. Cell Biol. *132*, 657–666.

Banani, S.F., Lee, H.O., Hyman, A.A., and Rosen, M.K. (2017). Biomolecular condensates: organizers of cellular biochemistry. Nat. Rev. Mol. Cell Biol. *18*, 285–298.

Boncoraglio, A., Minoia, M., and Carra, S. (2012). The family of mammalian small heat shock proteins (HSPBs): implications in protein deposit diseases and motor neuropathies. Int. J. Biochem. Cell Biol. *44*, 1657–1669.

Bryantsev, A.L., Chechenova, M.B., and Shelden, E.A. (2007). Recruitment of phosphorylated small heat shock protein Hsp27 to nuclear speckles without stress. Exp. Cell Res. *313*, 195–209.

Capanni, C., Del Coco, R., Squarzoni, S., Columbaro, M., Mattioli, E., Camozzi, D., Rocchi, A., Scotlandi, K., Maraldi, N., Foisner, R., and Lattanzi, G. (2008). Prelamin A is involved in early steps of muscle differentiation. Exp. Cell Res. *314*, 3628–3637.

Davidson, P.M., and Lammerding, J. (2014). Broken nuclei–lamins, nuclear mechanics, and disease. Trends Cell Biol. *24*, 247–256.

Davies, B.S., Coffinier, C., Yang, S.H., Barnes, R.H., 2nd, Jung, H.J., Young, S.G., and Fong, L.G. (2011). Investigating the purpose of prelamin A processing. Nucleus *2*, 4–9.

Dechat, T., Adam, S.A., Taimen, P., Shimi, T., and Goldman, R.D. (2010). Nuclear lamins. Cold Spring Harb. Perspect. Biol. *2*, a000547.

den Engelsman, J., Boros, S., Dankers, P.Y., Kamps, B., Vree Egberts, W.T., Böde, C.S., Lane, L.A., Aquilina, J.A., Benesch, J.L., Robinson, C.V., et al. (2009). The small heat-shock proteins HSPB2 and HSPB3 form well-defined heterooligomers in a unique 3 to 1 subunit ratio. J. Mol. Biol. *393*, 1022–1032.

Fernando, P., Kelly, J.F., Balazsi, K., Slack, R.S., and Megeney, L.A. (2002). Caspase 3 activity is required for skeletal muscle differentiation. Proc. Natl. Acad. Sci. USA *99*, 11025–11030.

Ganassi, M., Mateju, D., Bigi, I., Mediani, L., Poser, I., Lee, H.O., Seguin, S.J., Morelli, F.F., Vinet, J., Leo, G., et al. (2016). A surveillance function of the HSPB8-BAG3-HSP70 chaperone complex ensures stress granule integrity and dynamism. Mol. Cell *63*, 796–810.

Gilchrist, S., Gilbert, N., Perry, P., Ostlund, C., Worman, H.J., and Bickmore, W.A. (2004). Altered protein dynamics of disease-associated lamin A mutants. BMC Cell Biol. *5*, 46.

Gonzalez-Suarez, I., Redwood, A.B., Perkins, S.M., Vermolen, B., Lichtensztejin, D., Grotsky, D.A., Morgado-Palacin, L., Gapud, E.J., Sleckman, B.P., Sullivan, T., et al. (2009). Novel roles for A-type lamins in telomere biology and the DNA damage response pathway. EMBO J. *28*, 2414–2427.

Grose, J.H., Langston, K., Wang, X., Squires, S., Mustafi, S.B., Hayes, W., Neubert, J., Fischer, S.K., Fasano, M., Saunders, G.M., et al. (2015). Characterization of the cardiac overexpression of HSPB2 reveals mitochondrial and myogenic roles supported by a cardiac HspB2 interactome. PLoS ONE *10*, e0133994.

Ishiwata, T., Orosz, A., Wang, X., Mustafi, S.B., Pratt, G.W., Christians, E.S., Boudina, S., Abel, E.D., and Benjamin, I.J. (2012). HSPB2 is dispensable for the cardiac hypertrophic response but reduces mitochondrial energetics following pressure overload in mice. PLoS ONE *7*, e42118.

Jao, C.Y., and Salic, A. (2008). Exploring RNA transcription and turnover in vivo by using click chemistry. Proc. Natl. Acad. Sci. USA *105*, 15779–15784.

Kaufman, S.J., and Foster, R.F. (1988). Replicating myoblasts express a muscle-specific phenotype. Proc. Natl. Acad. Sci. USA *85*, 9606–9610.

Kolb, S.J., Snyder, P.J., Poi, E.J., Renard, E.A., Bartlett, A., Gu, S., Sutton, S., Arnold, W.D., Freimer, M.L., Lawson, V.H., et al. (2010). Mutant small heat shock protein B3 causes motor neuropathy: utility of a candidate gene approach. Neurology *74*, 502–506.

Lammerding, J., Fong, L.G., Ji, J.Y., Reue, K., Stewart, C.L., Young, S.G., and Lee, R.T. (2006). Lamins A and C but not lamin B1 regulate nuclear mechanics. J. Biol. Chem. *281*, 25768–25780.

Lamond, A.I., and Spector, D.L. (2003). Nuclear speckles: a model for nuclear organelles. Nat. Rev. Mol. Cell Biol. *4*, 605–612.

Larsen, B.D., Rampalli, S., Burns, L.E., Brunette, S., Dilworth, F.J., and Megeney, L.A. (2010). Caspase 3/caspase-activated DNase promote cell differentiation by inducing DNA strand breaks. Proc. Natl. Acad. Sci. USA *107*, 4230–4235.

Lees-Miller, S.P. (2006). Dysfunction of lamin A triggers a DNA damage response and cellular senescence. DNA Repair (Amst.) *5*, 286–289.

Liang, Y., Chiu, P.H., Yip, K.Y., and Chan, S.Y. (2011). Subcellular localization of SUN2 is regulated by lamin A and Rab5. PLoS ONE *6*, e20507.

Lourim, D., and Lin, J.J. (1992). Expression of wild-type and nuclear localization-deficient human lamin A in chick myogenic cells. J. Cell Sci. *103*, 863–874.

Mariappan, I., and Parnaik, V.K. (2005). Sequestration of pRb by cyclin D3 causes intranuclear reorganization of lamin A/C during muscle cell differentiation. Mol. Biol. Cell *16*, 1948–1960.

Markiewicz, E., Venables, R., Alvarez-Reyes, M., Quinlan, R., Dorobek, M., Hausmanowa-Petrucewicz, I., and Hutchison, C. (2002). Increased solubility of lamins and redistribution of lamin C in X-linked Emery-Dreifuss muscular dystrophy fibroblasts. J. Struct. Biol. *140*, 241–253.

Markiewicz, E., Ledran, M., and Hutchison, C.J. (2005). Remodelling of the nuclear lamina and nucleoskeleton is required for skeletal muscle differentiation in vitro. J. Cell Sci. *118*, 409–420.

Mattioli, E., Columbaro, M., Capanni, C., Maraldi, N.M., Cenni, V., Scotlandi, K., Marino, M.T., Merlini, L., Squarzoni, S., and Lattanzi, G. (2011). Prelamin A-mediated recruitment of SUN1 to the nuclear envelope directs nuclear positioning in human muscle. Cell Death Differ. *18*, 1305–1315.

Patel, A., Lee, H.O., Jawerth, L., Maharana, S., Jahnel, M., Hein, M.Y., Stoynov, S., Mahamid, J., Saha, S., Franzmann, T.M., et al. (2015). A liquid-to-solid phase transition of the ALS protein FUS accelerated by disease mutation. Cell *162*, 1066–1077.

Schmidt, H.B., and Rohatgi, R. (2016). In vivo formation of vacuolated multiphase compartments lacking membranes. Cell Rep. *16*, 1228–1236.

Shimi, T., Pfleghaar, K., Kojima, S., Pack, C.G., Solovei, I., Goldman, A.E., Adam, S.A., Shumaker, D.K., Kinjo, M., Cremer, T., and Goldman, R.D. (2008). The A- and B-type nuclear lamin networks: microdomains involved in chromatin organization and transcription. Genes Dev. *22*, 3409–3421.

Spann, T.P., Goldman, A.E., Wang, C., Huang, S., and Goldman, R.D. (2002). Alteration of nuclear lamin organization inhibits RNA polymerase II-dependent transcription. J. Cell Biol. *156*, 603–608.

Sudnitsyna, M.V., Mymrikov, E.V., Seit-Nebi, A.S., and Gusev, N.B. (2012). The role of intrinsically disordered regions in the structure and functioning of small heat shock proteins. Curr. Protein Pept. Sci. *13*, 76–85.

Sugiyama, Y., Suzuki, A., Kishikawa, M., Akutsu, R., Hirose, T., Waye, M.M., Tsui, S.K., Yoshida, S., and Ohno, S. (2000). Muscle develops a specific form of small heat shock protein complex composed of MKBP/HSPB2 and HSPB3 during myogenic differentiation. J. Biol. Chem. *275*, 1095–1104.

Sullivan, T., Escalante-Alcalde, D., Bhatt, H., Anver, M., Bhat, N., Nagashima, K., Stewart, C.L., and Burke, B. (1999). Loss of A-type lamin expression compromises nuclear envelope integrity leading to muscular dystrophy. J. Cell Biol. *147*, 913–920.

van den IJssel, P., Wheelock, R., Prescott, A., Russell, P., and Quinlan, R.A. (2003). Nuclear speckle localisation of the small heat shock protein alpha B-crystallin and its inhibition by the R120G cardiomyopathy-linked mutation. Exp. Cell Res. *287*, 249–261.

Verstraeten, V.L., Ji, J.Y., Cummings, K.S., Lee, R.T., and Lammerding, J. (2008). Increased mechanosensitivity and nuclear stiffness in Hutchinson-Gilford progeria cells: effects of farnesyltransferase inhibitors. Aging Cell *7*, 383–393.

Vos, M.J., Kanon, B., and Kampinga, H.H. (2009). HSPB7 is a SC35 speckle resident small heat shock protein. Biochim. Biophys. Acta *1793*, 1343–1353.

Wechsler, A.S., Entwistle, J.C., 3rd, Yeh, T., Jr., Ding, M., and Jakoi, E.R. (1994). Early gene changes in myocardial ischemia. Ann. Thorac. Surg. *58*, 1282–1284.

Zhu, L., and Brangwynne, C.P. (2015). Nuclear bodies: the emerging biophysics of nucleoplasmic phases. Curr. Opin. Cell Biol. *34*, 23–30.

Zhu, C.H., Mouly, V., Cooper, R.N., Mamchaoui, K., Bigot, A., Shay, J.W., Di Santo, J.P., Butler-Browne, G.S., and Wright, W.E. (2007). Cellular senescence in human myoblasts is overcome by human telomerase reverse transcriptase and cyclin-dependent kinase 4: consequences in aging muscle and therapeutic strategies for muscular dystrophies. Aging Cell *6*, 515–523.